A Probability Distribution Model-Based Approach for Foot Placement Prediction in the Early Swing Phase With a Wearable IMU Sensor

Xinxing Chen, *Member, IEEE*, Kuangen Zhang, *Graduate Student Member, IEEE*, Haiyuan Liu, Yuquan Leng, *Member, IEEE*, and Chenglong Fu, *Member, IEEE*

***Abstract*— Predicting the next foot placement of humans during walking can help improve compliant interactions between humans and walking aid robots. Previous studies have focused on foot placement estimation with wearable inertial sensors after heel-strike, but few have predicted foot placements in advance during the early swing phase. In this study, a Bayesian inference-based foot placement prediction approach was proposed. Possible foot placements were modeled as a probability distribution grid map. With selected foot motion feature events detected sequentially in the early swing phase, the foot placement probability map could be updated iteratively using the feature models we built. The weighted center of the probability distribution was regarded as the predicted foot placement. Prediction errors were evaluated with collected walking data sets. When testing with the data from inertial measurement units, the prediction errors were (5.46 cm ± 10.89 cm, −0.83 cm ± 10.56 cm) for cross-velocity walking data and (−4.99 cm ± 12.31 cm, −11.27 cm ± 7.74 cm) for cross-subject–cross-velocity walking data. The results were comparable to previous works yet the prediction could be made earlier. For the subject who walked with more stable gaits, the prediction error can be further decreased. The proposed foot placement prediction approach can be utilized to help walking aid robots adjust their pose before each heel-strike event during walking, which will make human–robot interactions more compliant. This study is also expected to inspire additional probabilistic gait analysis works.**

***Index Terms*— Human walking, inertial sensors, foot placement, Bayesian inference, gait prediction.**

Manuscript received July 13, 2021; revised October 18, 2021 and November 11, 2021; accepted November 12, 2021. Date of publication December 7, 2021; date of current version December 21, 2021. This work was supported in part by the National Natural Science Foundation of China under Grant U1913205, Grant 62103180, Grant 52175272, and Grant 51805237; in part by the National Key Research and Development Program of China under Grant 2018YFC2001601; in part by the China Postdoctoral Science Foundation under Grant 2021M701577; in part by the Guangdong Basic and Applied Basic Research Foundation under Grant 2020B1515120098; in part by the Guangdong Innovative and Entrepreneurial Research Team Program under Grant 2016ZT06G587; in part by the Science, Technology and Innovation Commission of Shenzhen Municipality under Grant SGLH20180619172011638, Grant ZDSYS20200811143601004, and Grant KQTD20190929172505711; in part by the Stable Support Plan Program of Shenzhen Natural Science Fund under Grant 20200925174640002; in part by the Joint Fund of Science & Technology Department of Liaoning Province and State Key Laboratory of Robotics, China, under Grant 2020-KF-22-03; and in part by the Centers for Mechanical Engineering Research and Education at MIT and SUSTech. *(Corresponding author: Chenglong Fu.)*

This work involved human subjects or animals in its research. Approval of all ethical and experimental procedures and protocols was granted by the Southern University of Science and Technology (SUSTech) Medical Ethics Committee under Approval No. 20210009.

Xinxing Chen, Haiyuan Liu, Yuquan Leng, and Chenglong Fu are with the Shenzhen Key Laboratory of Biomimetic Robotics and Intelligent Systems, Shenzhen 518055, China, and also with the Guangdong Provincial Key Laboratory of Human-Augmentation and Rehabilitation Robotics in Universities, Southern University of Science and Technology, Shenzhen 518055, China (e-mail: fucl@sustech.edu.cn).

Kuangen Zhang is with the Shenzhen Key Laboratory of Biomimetic Robotics and Intelligent Systems, Shenzhen 518055, China, also with the Guangdong Provincial Key Laboratory of Human-Augmentation and Rehabilitation Robotics in Universities, Southern University of Science and Technology, Shenzhen 518055, China, and also with the Department of Mechanical Engineering, The University of British Columbia, Vancouver, BC V6T 1Z4, Canada.

This article has supplementary downloadable material available at https://doi.org/10.1109/TNSRE.2021.3133656, provided by the authors.

Digital Object Identifier 10.1109/TNSRE.2021.3133656

I. Introduction

EXOSKELETON robots [1]–[3] provide assistance to the human body by applying force directly to joints or limbs. However, it is difficult to design a controller to ensure that the assistance is consistent with the human gait. An unsuitable controller may even interfere with a human's autonomous walking. Predicting foot placement would improve the performance of walking aid robots (e.g. exoskeleton robots, supernumerary robotic limbs [4], [5], robotic prostheses [6] and cane-type walking-aid robots [7], [8]) as it would provide the robots with knowledge of the stride length and width in advance and help them adjust their pose before providing assistance. In this study, we aim to propose a probability distribution model-based approach to predict foot placement when people are walking on flat ground. The proposed method can serve as a solution for improving the compliance of human–robot interactions, and it can also inspire further applications of probabilistic methods in human motion prediction.

Human gait measurement and estimation are essential for falling risk assessment [9], disease diagnosis [10], etc., therefore there are increasing number of related studies in recent years. The mainstream human gait measurement methods include computer vision methods [11], which require external

cameras and may bring heavy computational loads, and motion trajectory tracking with small-size and low-cost inertial measurement units (IMUs). Hao *et al.* [12] used IMUs to build three-dimensional (3D) foot trajectories when a human is walking with a steady gait, and from the trajectories they estimated the stride length and width. Hannink *et al.* summarized some stride length estimation methods in [13] and found that the majority of methods had a similar mean accuracy, within 1 cm, and similar precision of approximately 6–8 cm.

Most of the existing work is focused on foot placement measurement. Typical foot placement measurement methods using IMUs [12], [14] rely on zero velocity update (ZUPT) which can only be conducted after the heel-strike event. However, for walking aid robots, predicting foot placement prior to heel-strike can prevent them from interfering with human walking and help them adjust to suitable poses to assist users [9], [15]. Thus, compared with foot placement measurement, foot placement prediction in advance is of greater significance for compliant human–robot interaction.

We conducted a literature review on foot placement prediction but found very limited related work. Zhang *et al.* [16] predicted foot placements by fusing sequential 3D gaze and environmental context when subjects were walking on rough terrain with constrained footholds. With the user-dependent time window and environmental context, the prediction error was approximately 8.6 cm, but the error could exceed 18 cm when the method was working without the environmental context. Sahoo *et al.* [17] predicted human's step length with adaptive neural fuzzy inference system (ANFIS) using an IMU mounted on the thigh. The walking dataset was collected with fixed step lengths and the performance of the method with various walking speeds and gaits remains to be evaluated. The average angular velocity of the thigh during the swing phase was used as an input of ANFIS, which can only be calculated just before the heel-strike event and makes it hard to conduct a real "prediction" in advance. When the proposed ANFIS was tested on two unseen fixed step lengths, the root mean square error (RMSE) was approximately 5 to 6 cm. Wang and Srinivasan [18] proposed that the next foot placements can be fitted with the motion state of the pelvis, which is consistent with the conclusion of [19] that the foot placement is relevant to the motion state of the center of mass (CoM), but the prediction error was not analyzed quantitatively. The authors of [18] found that the pelvis state, instead of the swing foot state, was the dominant explainer of future foot placements at the mid-stance phase, because most swing foot deviation typically happens after mid-stance. However, it is difficult to measure the state of CoM with motion sensors such as IMUs because of the accumulated sensor drift [20]. Instead, it is easier to estimate the motion state of the foot with IMU data corrected with ZUPT methods [12], [21].

The Bayesian inference method is a good solution for streaming data prediction on the premise that there is a clear probabilistic model for the measured data and the parameter to be predicted [22]. It has been widely applied in robotic environment perception [23], [24] and human motion recognition [25]. However, it has not been used to predict human foot placement quantitatively because of the lack of a probabilistic model between human gait parameters and motion features.

In this study, a Bayesian inference-based foot placement prediction approach was proposed using the swing foot motion state features in the early swing phase. Walking data of 7 subjects was collected, including multiple speeds (0.5∼1.4 m/s) and many different gaits. Using the collected data, a few foot motion state features and their relationship with foot placements were investigated. Feature models were built with a part of the data for the selected features and further used to update the foot placement probability map. To evaluate the performance of the proposed method, we tested it offline on the collected IMU data with left-out speeds and left-out subjects. The RMSEs of the prediction results along the walking direction and horizontally perpendicular to the walking direction are (12.18 cm, 10.58 cm) for cross-velocity walking data, and (13.28 cm, 13.67 cm) for cross-subject–cross-velocity walking data. For one of the subject who walked with more stable and regular gaits, the RMSEs can be reduced to (5.77 cm, 6.89 cm). The proposed approach can be applied to various subjects with various walking speeds. Compared with previous methods that predicted foot placements in the late swing phase, the proposed method can make the prediction earlier and achieve similar accuracy.

The main contribution of the study is the proposal of a probability distribution-based foot placement prediction approach that can make predictions in the first 50% of the swing phase. A Bayesian inference-based approach was firstly adopted to quantitatively infer the next foot placement.

In terms of sensing technology, the IMU, which was typically used to measure past and current motion signals, is applied to predict future foot placement in this paper. Foot motion state features can be detected by IMU and serve as events triggering the update of the probability map.

In terms of foot motion state feature modeling, a few foot motion features in the early swing phase are investigated. Their relationship with foot placements are modeled in this paper, which are rarely seen in literatures. These models are expected to play a role in further human walking gait studies.

The rest of this paper is organized as follows. In Section II, the Bayesian inference-based foot placement prediction approach is introduced. Swing foot motion state feature selection and modeling are also presented. In Section III, the data collection process is introduced and the performance evaluation for the proposed approach is conducted. Section IV concludes the paper.

II. The Bayesian Inference-Based Foot Placement Prediction

A. Overview of the Proposed Approach

The proposed foot placement prediction approach consists of two main parts: (1) 3D foot trajectory estimation and feature extraction; and (2) foot placement probability distribution modeling and updating using Bayesian inference. The scheme of the proposed approach is illustrated in Fig. 1. To realize 3D foot trajectory estimation, a widely used integration method is adopted to process the acceleration data and the angular

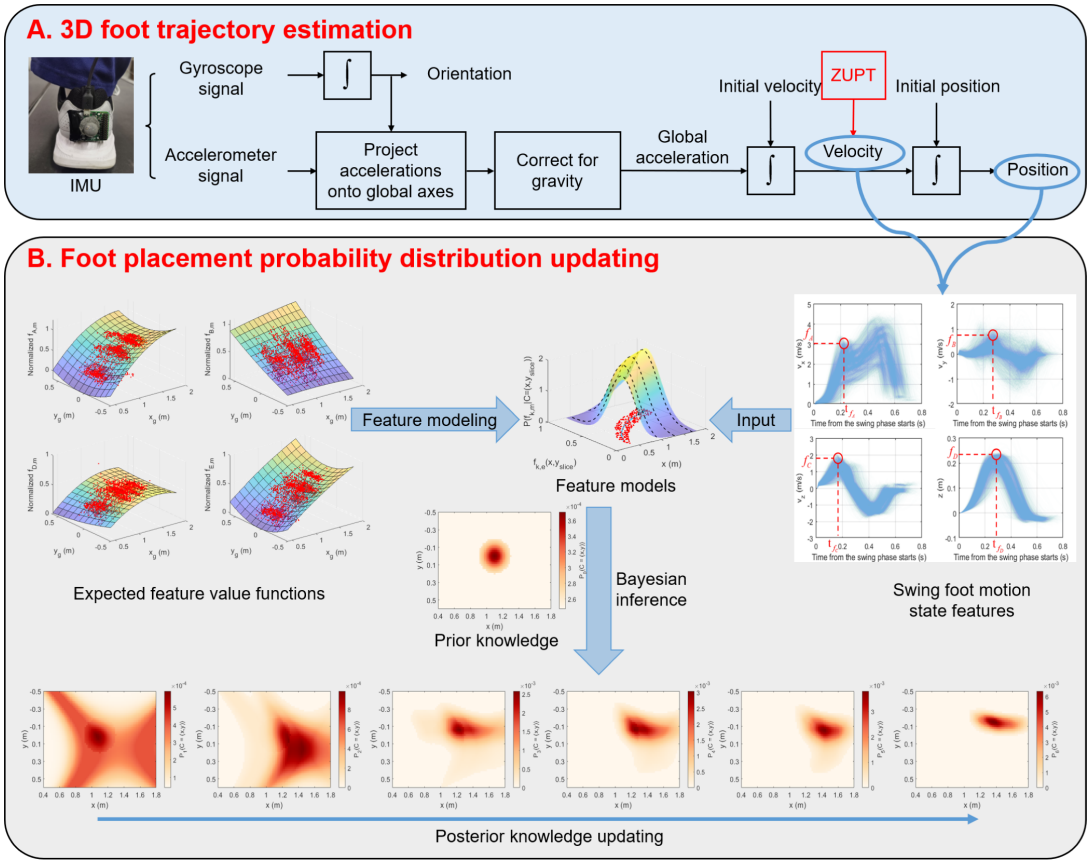

Fig. 1. A scheme of the proposed foot placement prediction approach. Part A illustrates the process of 3D foot trajectory estimation. Part B illustrates the update process of the foot placement probability distribution map. Expected feature value functions are fitted and further used to build the feature models. The estimated swing foot motion state features and the feature models are used in Bayesian inference to update the foot placement probability map.

velocity data collected by the IMU. A few features can be extracted from the foot trajectory and the motion state of the swing foot estimated from the streaming data captured by IMU. An area on the walking surface in front of the walking subject is modeled as a grid map. The prior knowledge of the foot placement probability distribution in the grid map is obtained through the estimated historic stride length and width. With the feature events detected sequentially, the probability distribution is updated iteratively using the feature models built in this paper. The weighted center of the probability distribution is considered as the predicted foot placement. In the following two subsections, the two parts are introduced in detail. The fourth subsection gives an example workflow of the proposed approach.

B. 3D Foot Trajectory Estimation

Foot trajectory estimation usually involves three main procedures: (1) orientation estimation, (2) velocity estimation, and (3) trajectory estimation. The gyroscope signals and the accelerometer signals are captured by an IMU attached to the heel of the subject. The gyroscope signals are integrated to obtain the angular orientation of the IMU. The Kalman filter was applied during this process to reduce the sensor drifting error. The velocity estimation first uses the obtained orientation to project accelerometer signals onto the global axes and then corrects for gravity. The global accelerations are integrated to obtain the linear velocities. Accumulated sensor drift may affect the estimation accuracy. ZUPT methods have been widely used to restrain the estimation error [12], [21]. Considering that the foot is stationary on the ground during stance phases, the foot velocity can be set to zero at this instant. The foot velocity profile in the previous swing phase can be corrected with linear corrections, which can further reduce drift errors [26]. Finally, the foot position is estimated by integrating linear velocities, and trajectory of the foot is reconstructed. The above process is illustrated in Part A of Fig. 1. Since foot trajectory estimation is not the main contribution of this paper, readers can refer to our previous paper [12] for more details.

With the estimated swing foot trajectory and velocity profile, the selected features in Section II-C1 can be detected from the data flow in each early swing phase by recording historic feature extremums.

C. Foot Placement Probability Distribution Modeling and Updating Using Bayesian Inference

1) Swing Foot Motion State Feature Selection: Although complete time-series foot positions in the whole swing phase during walking can be recorded by motion capture systems or IMUs, real-time foot placement prediction relies on streaming foot motion state data, and prediction is expected to be conducted in the early swing phase. Therefore, commonly

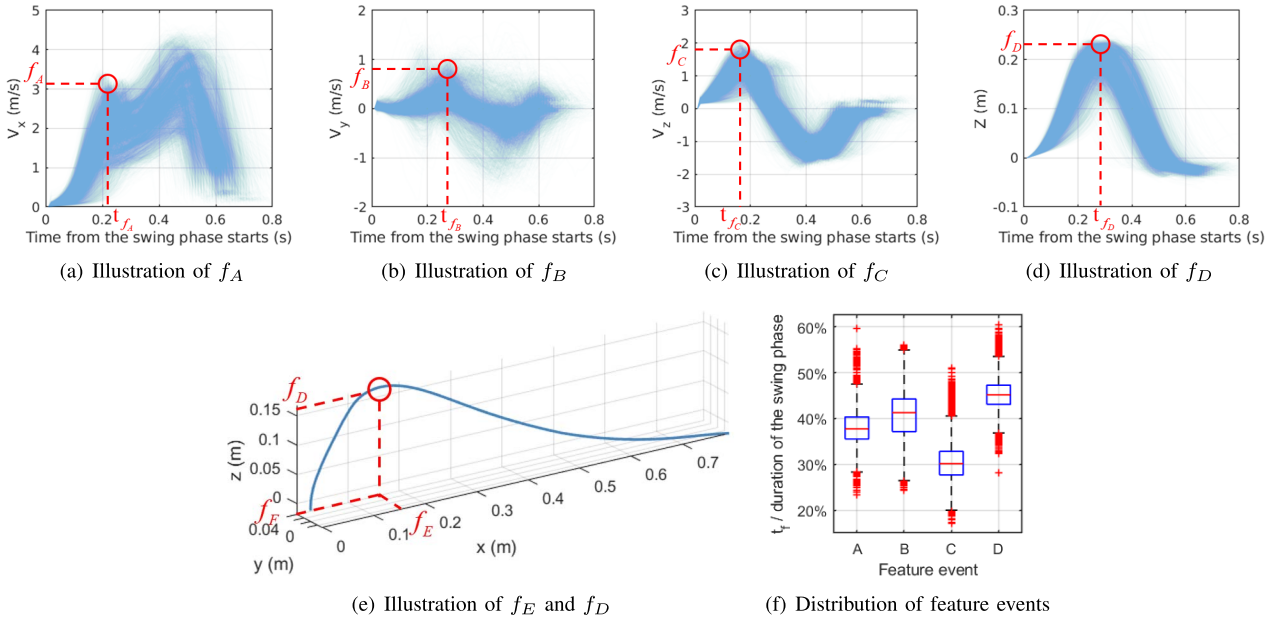

(a) Illustration of f_A (b) Illustration of f_B (c) Illustration of f_C (d) Illustration of f_D

(e) Illustration of f_E and f_D (f) Distribution of feature events

Fig. 2. Illustrations of features $f_A - f_F$ and the distribution of the feature events in the swing phase. (a)–(d) present the v_x, v_y, v_z, and z profiles in the swing phase of the 7403 steps. f_A–f_F present an example set of feature values. t_{f_A}–t_{f_D} refer to the time intervals from toe-off to the corresponding feature event. (f) shows the percentage of t_{f_A}–t_{f_D} in the swing phase duration.

used features in data prediction (e.g., mean and variance of time-series data) are not suitable for foot placement prediction. Instead, we have to investigate a few feature events that usually occur in the early swing phase and are easy to detect in the data flow.

According to [18] and [27], the motion state of the swing foot is related to the next foot placement no matter the subject is walking stably or trying to restore the balance. After comparing the correlation between the foot placements and multiple swing foot motion state features, six features were selected for further modeling and used in foot placement prediction. More details on feature selection are presented in the Supplementary Document attached with the paper. Let us define the coordinate system as: the origin is where the foot starts to swing, x axis is alone the walking direction, y axis is horizontally perpendicular to the walking direction, and z axis is perpendicular to the floor. The six selected features are: f_A: the first extremum of v_x; f_B: the first positive extremum of v_y; f_C: the first positive extremum of v_z; f_D: the largest offset of the heel along the z axis; f_E: the corresponding offset along the x axis when the heel reaches the highest position; and f_F: the corresponding offset along the y axis when the heel reaches the highest position. To investigate when these feature events typically occur during the swing phase, walking data of seven subjects were collected (details are presented in Section. III-A). The foot motion state profiles in 7403 steps are plotted in Fig. 2. The selected features are also illustrated. It can be seen from Fig. 2(f) that the top edges of the boxes are all below 50% swing phase and that all the outliers stay below 60%, which means that all these feature events can usually be detected in the early swing phase. Therefore, these features are suitable for the proposed foot placement prediction method.

2) Bayesian Inference-Based Foot Placement Prediction: The typical Bayesian inference workflow consists of three main steps [22]: capturing available knowledge about a parameter via the prior distribution, which is typically determined before data collection; determining the likelihood function using the information about the parameters available in the observed data; and combining both the prior distribution and the likelihood function using Bayes' theorem in the form of the posterior distribution. The posterior distribution reflects the updated knowledge about the parameter, balancing prior knowledge with observed data.

In this paper, it is assumed that the next foot placement $C = (x, y)$ of a walking subject will be always located within an area $\mathcal{A}$ on the ground in front of the subject. x and y refer to the offset of the heel along the walking direction (stride length) and horizontally perpendicular to the walking direction (stride width), respectively, from the toe-off event to the heel-strike event. The gait phases and the area $\mathcal{A}$ are illustrated in Fig. 3.

The area $\mathcal{A}$ is modeled as a grid map, of which the number of grid cells is $a \times b$. Before the toe-off event in a step, the prior knowledge about the next foot placement is vague. Although the uniform distribution is widely used as a prior distribution [22]–[24], in this paper, the historic foot placements also contribute to build the prior distribution because humans normally walk with bounded acceleration and jerk such that the difference of stride length and width between sequential steps is limited. Therefore, the prior probability distribution about the next foot placement is built as a Gaussian distribution with bias. The probability that the next foot placement will fall on the ith ($1 \leqslant i \leqslant a \times b$, $i \in Z$) grid cell is:

$$P_0\left(C = (x_i, y_i)\right) = \alpha_0\left(1 + \frac{\beta}{\sqrt{2\pi}\,\sigma}\exp\left(-\frac{(x_i - x_h)^2 + (y_i - y_h)^2}{2\sigma^2}\right)\right), \quad (1)$$

where x_i and y_i represent the position of grid cell i taking the toe-off position of the foot as the origin. β is a scaling factor

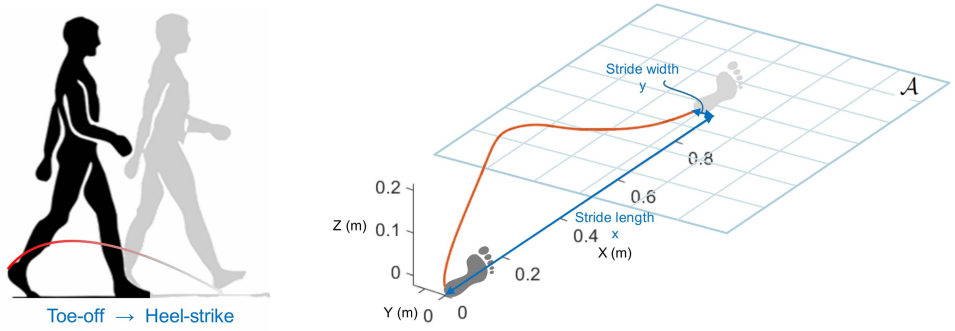

(a) Illustration of the toe-off event and the heel-strike event

(b) Illustration of the foot placement and the area $\mathcal{A}$ in front of the subject

Fig. 3. Illustrations of the gait events, the foot placement, and the area $\boldsymbol{\mathcal{A}}$. In (a), the person depicted with the darker color is at the toe-off event. After the person takes a stride, the person will turn to the heel-strike event when the swing foot contacts the ground. The red curve represents the swing foot trajectory. In (b), the darker footprint represents the foot placement at the toe-off event, while the lighter one represents the predicted foot placement at the next heel-strike event. The area $\boldsymbol{\mathcal{A}}$ is illustrated with a grid box.

adjusting the degree of uncertainty of the prior distribution and is set to be 0.5 in this paper. x_h and y_h are variables related to historic foot placements. In this study, they are defined as the average stride length and width in the previous two steps. α_0 acts as a normalizing factor to ensure the sum of the probability of all cells equals to 1, and can be calculated as:

$$\alpha_0 = \frac{1}{\sum_{i=1}^{a\times b}\left(1+\frac{\beta}{\sqrt{2\pi}\sigma}\exp\left(-\frac{(x_i-x_h)^2+(y_i-y_h)^2}{2\sigma^2}\right)\right)}. \quad (2)$$

Noting that selected feature events (introduced in Section II-C1) can be detected sequentially during the swing phase, the posterior distribution of the next foot placement can be updated according to Bayes' rule:

$$P_n(C=(x_i,y_i)|f_{n,m},f_{n-1,m}\dots f_{1,m}) = \alpha_n\cdot P(f_{n,m}|C=(x_i,y_i))\cdot P_{n-1}, \quad (3)$$

where $1\leqslant n\leqslant N$, $n\in Z$. N refers to the total number of selected features and is equal to 6 in this study. n refers to the sequence of the detected feature events. $f_{n,m}$ represents the measured value of the nth detected feature. P_{n-1} refers to the posterior probability after the $(n-1)$th iteration and acts as the prior probability in the nth iteration. P_0 can be calculated using Eq. (1). α_n acts as a normalizing factor to keep $\sum_{i=1}^{a\times b} P_n(C=(x_i,y_i)|f_{n,m},f_{n-1,m}\dots f_{1,m})=1$.

To achieve the iterative probability update in Eq. (3), "feature models" $P(f_{n,m}|C=(x_i,y_i))$ have to be built for all selected features. From the collected motion capture data set, we are able to conduct curve fitting on the measured feature values $(f_{A,m},f_{B,m},f_{C,m},f_{D,m},f_{E,m},f_{F,m})$ versus the foot placements $\boldsymbol{C}_g=(x_g,y_g)$. The walking data of subjects $1-4$ with walking speeds of 0.5 m/s, 1.0 m/s, and 1.4 m/s are utilized in curve fitting. All the measured feature values are normalized to $[0,1]$ with the upper-lower-bound normalizing method [28]. The normalized feature values are fitted into the quadratic polynomial functions of x_g and y_g (shown in Fig. 4). These functions are called "expected feature value functions" in this paper. It can be seen from Fig. 4 that there is a clear correlation between the next foot placement and the selected features, therefore the selected features can be utilized to infer foot placements. The correlation coefficients are presented in Section 1 of the Supplementary Document. The expected feature values $(f_{A,e},f_{B,e},f_{C,e},f_{D,e},f_{E,e},f_{F,e})$ calculated with the fitted functions for each grid cell (x_i,y_i) and the RMSE $(\gamma_A,\gamma_B,\gamma_C,\gamma_D,\gamma_E,\gamma_F)$ of the fitted functions are used to build the feature model. Assuming the next foot placement will fall at grid cell (x_i,y_i), the expected value of feature j $(j=A,B\dots F)$ is $f_{j,e}(x_i,y_i)$. Then the feature model assumes that the measured value of feature j follows the Gaussian distribution $N(f_{j,e}(x_i,y_i),\gamma_j^2)$. The feature model of feature j can be expressed as:

$$P(f_{j,m}|C=(x_i,y_i)) = \frac{1}{\sqrt{2\pi}\gamma_j}\exp\left(-\frac{(f_{j,m}-f_{j,e}(x_i,y_i))^2}{2\gamma_j^2}\right). \quad (4)$$

An more intuitional illustration of the feature model is presented in Section 2 of the Supplementary Document. The feature models will remain fixed throughout the prediction process. At each probability map updating iteration, Eq. (4) is calculated for the detected feature. After the last iteration $(n=N)$, the weighted center of the probability distribution is regarded as the predicted foot placement $\hat{C}=(\hat{x},\hat{y})$, that is:

$$(\hat{x},\hat{y}) = \sum_{i=1}^{a\times b}(x_i,y_i)\cdot P_N(C=(x_i,y_i)|f_{N,m},\dots f_{1,m}). \quad (5)$$

D. Demonstration of Foot Placement Prediction Workflow

In this subsection, an example iteration process for the probability map updating in one step is shown to demonstrate the foot placement prediction workflow more clearly.

The size of area $\mathcal{A}$ is set to be 1.4 m $\times$ 1.1 m, which can cover all the sampled foot placements. The grid size is 0.02 m. Before the swing phase of the subject's right foot, the prior probability distribution in $\mathcal{A}$ can be calculated by Eq. (1), where (x_h,y_h) are the average foot placements in the previous two steps. The prior probability distribution is shown in Fig. 5(a) as a normalized 2D Gaussian distribution. Then the right foot starts to swing until the first feature event

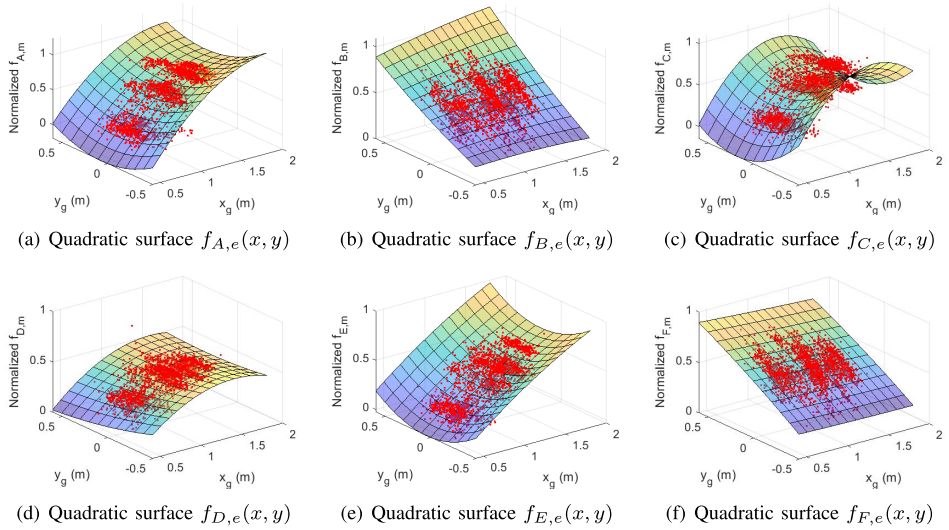

(a) Quadratic surface $f_{A,e}(x, y)$ (b) Quadratic surface $f_{B,e}(x, y)$ (c) Quadratic surface $f_{C,e}(x, y)$

(d) Quadratic surface $f_{D,e}(x, y)$ (e) Quadratic surface $f_{E,e}(x, y)$ (f) Quadratic surface $f_{F,e}(x, y)$

Fig. 4. Illustrations of expected feature value functions $f_{j,e}(x, y)$, $j = A, B \ldots F$. In (a)–(f), the red dots refer to sampled (x_g, y_g, normalized $f_{j,m}$). The surfaces are the quadratic fitting results for the sampled data, that is, the expected feature functions.

is detected, that is, v_z reaches its positive extrumem $f_{C,m}$, which is also denoted by $f_{1,m}$. Using Eq. (4) and (3), the probability map $P_1(C = (x_i, y_i)|f_{1,m})$ can be calculated (see Fig. 5(b)). During the swing phase, the extrumem of v_x, v_y and the maximum z is detected in sequence, and the probability map is updated iteratively with $f_{A,m}$, $f_{B,m}$, $f_{D,m}$,$f_{E,m}$, and $f_{F,m}$ (see Fig. 5(c)-5(g)). It should be noted that since the update of the probability map is triggered by detected feature events, there is not a fixed time interval between iterations.

In Fig. 5(g), the weighted center of the probability map is considered as the predicted foot placement, that is, $(\hat{x}, \hat{y}) = (1.4223 \text{ m}, -0.1414 \text{ m})$. According to the motion capture data, the ground truth foot placement is $(x_g, y_g) = (1.3964 \text{ m}, -0.1156 \text{ m})$. The distance error is (0.0259 m, −0.0258 m). The computational complexity is analyzed in Section 3 of the Supplementary Document.

III. Data Collection and Performance Evaluation

To conduct performance evaluation for the proposed approach, walking data of different subjects were collected. The experimental setup and data collection settings will be introduced in the following subsections. A motion capture data set and an IMU data set were collected. Using the motion capture data set, the ground truth trajectory of the right foot was built. With the swing foot trajectory and the foot velocity profile during the swing phase in each step, the selected features were extracted for foot placement prediction. The performance of the proposed approach was evaluated on the collected walking data set offline. Section III-C evaluates the approach with only the motion capture data. Section III-D tests the foot placement prediction approach with the IMU data.

A. Walking Data Collection: Subjects Walked With Various Gaits

Seven healthy adult subjects of various genders, heights, weights, and ages were recruited on campus to collect walking data. Data collection was approved and performed under the supervision of the Sustech Medical Ethics Committee (approval number: 20210009, date: 2021/3/2). Sufficient safety measures were taken to prevent any possible injuries during data collection.

An IMU (XSENS MTi-1s-DEV) was attached to the right heel of each subject while they were walking on a treadmill (shown in Fig. 6). The IMU was attached at the heel for two reasons. One reason is that the influence of the error associated with the zero-velocity assumption is minimized at this position [12], [29]. The second reason is that the acceleration and orientation information at the heel can be better utilized to detect the heel-strike event and divide the stance phase and the swing phase. The coordinate system is shown in Fig. 6(a). The X axis is oriented along the walking direction, and the Y axis and Z axis are horizontally and vertically perpendicular to the walking direction, respectively. The IMU collected the angular velocity and acceleration of the right foot with a sampling rate of 100 Hz. A motion capture system (Motion Analysis Raptor-12, sampling rate: 120 Hz) with 12 cameras was arranged around the data collection working space. A marker that could be captured by the motion capture system was attached close to the IMU on the right heel of each subject. The ground truth position of each subject's right foot was recorded in this way for further analysis and modeling.

To further test the performance of the proposed algorithm on different subjects and walking speeds, four out of the seven subjects were instructed to walk at speeds of 0.5 m/s, 0.8 m/s, 1.0 m/s, 1.2 m/s, and 1.4 m/s (Setting A). The other subjects were instructed to walk at speeds of 0.6 m/s, 0.7 m/s, 0.9 m/s, 1.1 m/s, and 1.3 m/s (Setting B). Details of the subjects and their walking velocity settings are shown in Table I. Data collection lasted for 260 s for each walking velocity. To synchronize the data captured by the IMU and the motion capture system, a stamping-foot action was conducted by the subjects before they started walking, during which the highest foot position can be captured by both the IMU and the motion capture system. The clock of the IMU and the motion capture system can then be synchronized by aligning the

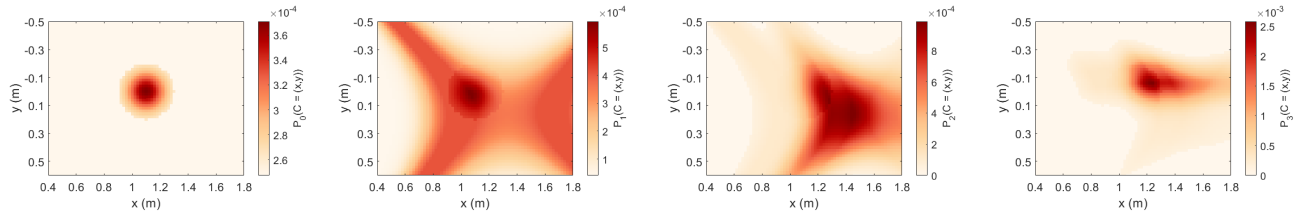

(a) Probability distribution P_0 (b) Probability distribution P_1 (c) Probability distribution P_2 (d) Probability distribution P_3

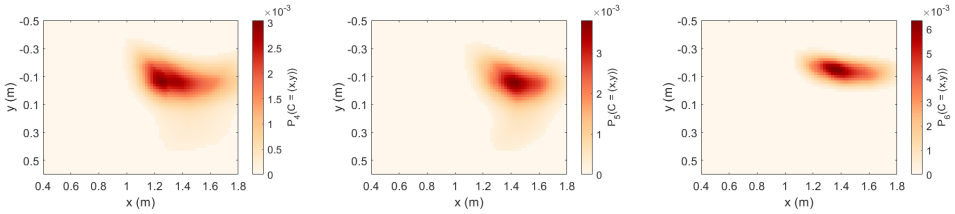

(e) Probability distribution P_4 (f) Probability distribution P_5 (g) Probability distribution P_6

Fig. 5. The updating process of the probability map. The coordinate system is the same as in Fig. 3(b). The color of each grid cell represents the probability that the next foot placement will fall on it.

(a) The treadmill and the coordinate system (b) The motion capture marker and IMU are attached to the right heel of a subject

Fig. 6. Illustrations of the data collection experimental setup.

TABLE I
DETAILS OF SEVEN SUBJECTS AND THE VELOCITY SETTINGS

No.	Gender	Height (cm)	Weight (kg)	Age	Velocity setting
1	Female	164	53	27	A
2	Female	158	55	23	A
3	Male	173	66	25	A
4	Male	188	75	22	A
5	Female	160	45	24	B
6	Male	184	70	24	B
7	Female	170	63	24	B

corresponding time. All the subjects were instructed to walk with various gaits, including long-stride, jog, split-stepping, cross-step, etc., while walking on the treadmill as long as they felt safe.

B. Motion Capture Data Processing

Interpolation has been conducted on the motion capture data to keep the time interval the same as the IMU data. The motion capture data set consisted of the ground truth position of the subjects' right heel $(\boldsymbol{x}_{m,0}, \boldsymbol{x}_{m,1} \ldots \boldsymbol{x}_{m,T})$ while they were walking on the treadmill (T refers to the timestamp when the subjects stopped walking). The data set was processed offline with the following steps: (1) treadmill velocity compensation, and (2) swing phase extraction.

Because the treadmill was rolling backwards with a preset velocity v_w along the X axis while the subjects were walking, the right heel velocity and position at each timestamp t should be compensated using Eq. (6) and Eq. (7).

$$\boldsymbol{v}_t = \frac{\boldsymbol{x}_{m,t} - \boldsymbol{x}_{m,t-1}}{\Delta t} + (v_w, 0, 0)^{\mathrm{T}}, \tag{6}$$

$$\boldsymbol{x}_t = \boldsymbol{v}_t \Delta t, \tag{7}$$

where $\boldsymbol{v}_t = (v_{x,t}, v_{y,t}, v_{z,t})^{\mathrm{T}}$ and $\boldsymbol{x}_t = (x_t, y_t, z_t)^{\mathrm{T}}$ are the compensated heel velocity vector and position vector, respectively. Δt is the time interval between two sequential timestamps.

With the compensated velocity and position, the swing phase and stance phase of the subjects' right foot were detected with a threshold method. In this study, only the foot trajectory in the early swing phase was used to predict foot placements, therefore we extracted the compensated heel velocity and position in each swing phase of the subjects' right foot. From the raw motion capture data set, we finally obtained a postprocessed data set, which consisted of the heel position and velocity in the right foot swing phase in 7403 steps. For each step, the ground truth foot placement position $\boldsymbol{C}_g = (x_g, y_g)$ was calculated by Eq. (8):

$$\boldsymbol{C}_g = (x_{t_{\mathrm{end}}}, y_{t_{\mathrm{end}}})^{\mathrm{T}} - (x_{t_{\mathrm{start}}}, y_{t_{\mathrm{start}}})^{\mathrm{T}}, \tag{8}$$

where t_{start} and t_{end} refer to the timestamps when the right foot starts to swing and switches to the stance phase, respectively.

The foot placements in these 7403 steps are shown in Fig. 7. It can be seen that the distribution of foot placements in our collected data sets has great randomness and variance because the subjects were instructed to walk with various gaits, which differed from any previous foot placement measurement/prediction work we reviewed in the Introduction. The randomness and variance of gaits bring significant difficulties to foot placement prediction.

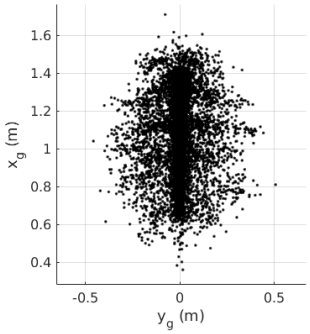

Fig. 7. Foot placements of 7403 steps in the postprocessed motion capture data set. The black dots represent the foot placements.

C. Prediction With the Motion Capture Data

In order to eliminate the influence of sensor drift and evaluate the Bayesian inference based method itself, we first tested the method on the collected motion capture data. The foot motion state features were all extracted from the captured foot motion trajectory.

Considering that the feature models introduced in Section II-C were built with the walking data of subjects $1-4$ with 0.5 m/s, 1.0 m/s, and 1.4 m/s walking speeds, two tests were conducted to test the universality of the proposed algorithm. The first test was the "cross-velocity" test, in which the method was tested on the walking data of subjects $1-4$ with 0.8 m/s and 1.2 m/s walking speeds. The second test was the "cross-subject–cross-velocity" test, in which the method was tested on the walking data of subject $5-7$ with 0.6 m/s, 0.7 m/s, 0.9 m/s, 1.1 m/s, and 1.3 m/s walking speeds. The prediction results are shown in Table II.

It can be seen that for Test 1, the mean prediction errors of $\hat{x}$ and $\hat{y}$ were within 0.5 cm, and the RMSEs were 10.32 cm and 8.85 cm, respectively. These results are comparable to the results in [17], which used a method that could only predict foot placements just before the heel-strike event, and the results in [16], which used additional environmental context. The prediction error is also of a similar dimension to some previous works on gait parameter measurement/estimation [13]. Scatter plots of the ground truth and the predicted foot placements are shown in Fig. 8(a) and (b). Blue dashed lines depict unity slopes, which represent perfect predictions. The scattered points $(x_g, \hat{x})$ and $(y_g, \hat{y})$ are linear fitted into the orange lines. It can be seen that in Test 1, there are some gaps between the linear fitting of $(x_g, \hat{x})$ and the unity slope because of the irregular gait change in the walking data collection process. The linear fitting of $(y_g, \hat{y})$ matches the unity slope well but still has some variance since most swing foot deviation typically happens during the late swing phase [18]. It should be noted that the subjects were instructed to take intentionally irregular gaits during walking, which could make the motion pattern in each separate step much different from our modeling and thus lead to prediction errors.

Subject 5-7 was also instructed to walk with various gaits, but their own walking patterns were different from the feature models built from the walking data of subject 1-4. Therefore, the RMSEs in Test 2, 13.00 cm and 12.39 cm for foot placement x and y, were higher than those in Test 1. The absolute values of the mean errors of x and y were also higher than those in Test 1, which can be explained by the cross-subject gait differences. Some interesting results that should be noted is that the RMSEs of subject 5, who walked with a more stable and regular gaits than others, are 6.29 cm and 5.42 cm on x and y, respectively.

Overall, without additional environmental context, the proposed algorithm can achieve foot placement prediction in the early swing phase, which is earlier than existing research [17] yet has comparable prediction errors. The proposed foot placement prediction method can be applied to various subjects and various walking speeds. For subjects who walk with stable and regular gaits, which are more commonly seen in reality, the RMSE of prediction can be further decreased.

TABLE II
PREDICTION ERROR OF x AND y ON THE MOTION CAPTURE DATA SET

Test	Error on x (cm)			Error on y (cm)		
	Mean	SD	RMSE	Mean	SD	RMSE
1	0.17	10.18	10.32	0.50	8.83	8.85
2	-8.14	10.14	13.00	-10.16	7.10	12.39

$*$ Test 1 refers to the "cross-velocity" test. Test 2 refers to the "cross-subject–cross-velocity" test.

TABLE III
PREDICTION ERROR OF x AND y ON THE IMU DATA SET

Test	Error on x (cm)			Error on y (cm)		
	Mean	SD	RMSE	Mean	SD	RMSE
1	5.46	10.89	12.18	-0.83	10.56	10.58
2	-4.99	12.31	13.28	-11.27	7.74	13.67

D. Prediction With the IMU Data

To demonstrate that the proposed foot placement prediction approach can also work with the IMU data, which contains noise and accumulated sensor drift, the collected IMU data, instead of the motion capture data, were utilized to extract selected features and update the probability map. We used a real-time integration of the foot motion in the swing phase to extract features. Once the swing foot contact the ground, ZUPT was conducted to make sure the foot would start from zero velocity in the next step. The motion capture data only provided the ground truth (x_g, y_g) for performance evaluation.

The reliability of using the feature values extracted from the IMU to predict foot placement were analyzed in Section 4 of the Supplementary Document. With the feature values estimated from the real-time integration of IMU data, the foot placement errors were calculated and shown in Table III. It can be seen that both the mean errors and the RMSEs were larger than the prediction error in Table II, which is in accordance with our expectations because of unavoidable sensor noise. But the prediction errors were still within a reasonable range and still comparable to existing works.

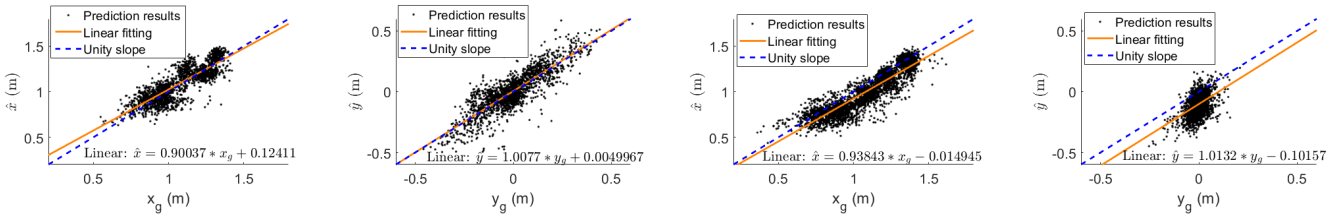

(a) Comparision between $\hat{x}$ and x_g in test 1 (b) Comparision between $\hat{y}$ and y_g in test 1 (c) Comparision between $\hat{x}$ and x_g in test 2 (d) Comparision between $\hat{y}$ and y_g in test 2

Fig. 8. Prediction results on the motion capture data. The x axis is the ground truth foot placement. The y axis is the predicted foot placement. The black dots are the prediction results. The blue dashed line is the unity slope, and the orange line is the linear fitting of the prediction results.

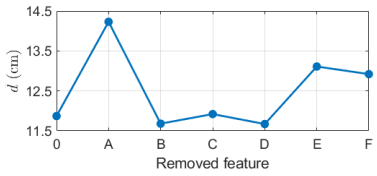

Fig. 9. The mean distance error $\bar{d}$ when removing any one of the selected features. 0 means using all the six features. A - F means removing $f_A - f_F$, respectively.

TABLE IV
PREDICTION ERROR ON THE IMU DATA SET USING FOUR FEATURES

Test	Error on x (cm)			Error on y (cm)		
	Mean	SD	RMSE	Mean	SD	RMSE
1	-5.90	10.25	11.82	-8.33	7.34	11.10
2	-2.77	11.24	11.58	-9.57	8.06	12.51

E. How Do Features Affect the Prediction Results?

It has to be admitted that there are differences on the gait pattern between various subjects and walking speeds, which may lead to biased feature modeling and unsatisfactory results. Therefore, we further studied how the accuracy of the proposed algorithm will be affected when removing any one of $f_A - f_F$. The resulting mean distance errors $\bar{d}$ were calculated for test 1 using the motion capture data and presented in Fig. 9.

It can be seen from Fig. 9 that removing feature f_A, f_C, f_E and f_F resulted in a higher $\bar{d}$, which reflected a substantial contribution of these four features. On the other hand, removing feature f_B and f_D resulted in a lower $\bar{d}$. These results may due to the biased feature modeling brought by the irregular and unstable gaits. According to these results, removing feature f_B and f_D and only using the other four features should improve the prediction accuracy. We tested the method with four features on the IMU data set and presented the results in Table IV. It can be seen that the accuracy was further improved in Test 2. These results verify that removing features with modeling bias could promote the prediction accuracy on data set with different gait patterns. But it does not mean that removing f_B and f_D can always substantially improve the accuracy. On data sets with less modeling bias (e.g. Test 1), the prediction accuracy may decrease with the reduction of features – the RMSE on y in Test 1 increased compared to that in Table III. Our suggestions for applying the method in this situation are: if the prediction accuracy on y is more important, keep all the features. If the accuracy on x or the short computation time is more important, f_B and f_D may be removed.

IV. DISCUSSIONS ON FURTHER APPLICATION

A. Application Potential on Walking-Aid Robots

In this paper, the foot placement prediction is made using the data from the first 50% of the swing phase, which means that the corresponding actions of the walking-aid robot should be conducted within the second 50% of the swing phase before foot contact. It may raise a concern whether this short duration is sufficient for a robotic device. The answer is yes. According to Fig. 2 in the manuscript, a swing phase lasts around 0.7 s, of which the second 50% should be around 0.35 s. Previous researches on robotic control [30], [31] reported that sliding mode control can realize fast tracking in such a short time (e.g., in [30], after unknown external disturbances, the 2-DOF lower-limb exoskeleton's velocity tracking error can coverage to 0 in 0.15 s). Therefore, the second 50% of the swing phase should be a sufficient buffer time for walking aid robots to adjust their motion state to support their users.

In terms of the prediction accuracy, in the "cross-velocity–cross-subject" test on the IMU data set, the proportional distance error was 9.71%, and the mean absolute distance error was 13.51 cm. Despite that there are limited literatures on foot placement prediction, and that the minimum accuracy required for a walking-aid robot remains to be studied, we believe foot placement prediction error less than 10% of the foot displacement can make sense to predict a rough range of possible foot placements. This rough range should be enough for typical walking-aid robots (e.g., exoskeletons and robotic prostheses) to estimate the terrain type for the next step and adjust their pose and stiffness [32].

B. Expansion of Foot Placement Prediction

The proposed method may be expanded to make further foot placement prediction, such as the height of foot placement on ramps or stairs, and the orientation of the foot. The models between the foot placement (x, y, z), the foot orientation, and the feature values can be built in the same way as this paper did. The probability distribution will be of higher dimension depend on the number of parameters being predicted. But it should be noted that maintaining higher-dimensional probability distributions leads to high computational cost. Decoupling the dimensions, that is, replacing

the high-dimensional probability distribution with a few low-dimensional distributions can help reducing the computational complexity.

V. Conclusion

This study demonstrates a probability distribution model-based approach for foot placement prediction. This approach can make predictions in the early swing phase (i.e., first 50% of the swing phase) by modeling possible foot placements as a probability distribution map and updating the map with selected foot motion features, which can be detected sequentially in the early swing phase. The two main contributions of this study are as follows: (1) Foot motion features and their relationship with foot placements were studied and modeled; and (2) Using the feature models, a Bayesian inference foot placement prediction method was formulated. The proposed approach can be applied to various subjects with various walking speeds. Compared with methods of previous works, which predicted foot placements in the late swing phase, the proposed method can make the prediction earlier and achieve similar accuracy. The RMSEs of the prediction results were (12.18 cm, 10.58 cm) for the cross-velocity test and (13.28 cm, 13.67 cm) for the cross-subject–cross-velocity test.

The proposed foot placement prediction approach can help walking aid robots adjust their pose before each heel-strike event during walking, which will make human–robot interactions more compliant. This study is also expected to inspire additional probabilistic gait analysis works.

Future work will focus on user-adaptive online feature modeling and adapting the foot placement prediction method to patients walking with abnormal gaits.

References

[1] Z. Li, Z. Ren, K. Zhao, C. Deng, and Y. Feng, "Human-cooperative control design of a walking exoskeleton for body weight support," *IEEE Trans. Ind. Informat.*, vol. 16, no. 5, pp. 2985–2996, May 2020.

[2] Z. Li *et al.*, "Human-in-the-loop control of a wearable lower limb exoskeleton for stable dynamic walking," *IEEE/ASME Trans. Mechatronics*, vol. 26, no. 5, pp. 2700–2711, Oct. 2021.

[3] J. Huang, W. Huo, W. Xu, S. Mohammed, and Y. Amirat, "Control of upper-limb power-assist exoskeleton using a human-robot interface based on motion intention recognition," *IEEE Trans. Autom. Sci. Eng.*, vol. 12, no. 4, pp. 1257–1270, Oct. 2015.

[4] M. Hao, J. Zhang, K. Chen, and C. Fu, "Design and basic control of extra robotic legs for dynamic walking assistance," in *Proc. Int. Conf. Adv. Robot. Social Impacts (ARSO)*, 2019, pp. 246–250.

[5] B. Yang, J. Huang, X. Chen, C. Xiong, and Y. Hasegawa, "Supernumerary robotic limbs: A review and future outlook," *IEEE Trans. Med. Robot. Bionics*, vol. 3, no. 3, pp. 623–639, Aug. 2021.

[6] K. Zhang *et al.*, "Environmental features recognition for lower limb prostheses toward predictive walking," *IEEE Trans. Neural Syst. Rehabil. Eng.*, vol. 27, no. 3, pp. 465–476, Mar. 2019.

[7] Q. Yan, J. Huang, Z. Yang, Y. Hasegawa, and T. Fukuda, "Human-following control of cane-type walking-aid robot within fixed relative posture," *IEEE/ASME Trans. Mechatronics*, early access, Mar. 23, 2021, doi: 10.1109/TMECH.2021.3068138.

[8] S. Nakagawa *et al.*, "Tandem stance avoidance using adaptive and asymmetric admittance control for fall prevention," *IEEE Trans. Neural Syst. Rehabil. Eng.*, vol. 24, no. 5, pp. 542–550, May 2016.

[9] P. Di *et al.*, "Fall detection and prevention control using walking-aid cane robot," *IEEE/ASME Trans. Mechatronics*, vol. 21, no. 2, pp. 625–637, Apr. 2016.

[10] B. Mariani, M. C. Jiménez, F. J. G. Vingerhoets, and K. Aminian, "On-shoe wearable sensors for gait and turning assessment of patients with Parkinson's disease," *IEEE Trans. Biomed. Eng.*, vol. 60, no. 1, pp. 155–158, Jan. 2013.

[11] K.-D. Ng, S. Mehdizadeh, A. Iaboni, A. Mansfield, A. Flint, and B. Taati, "Measuring gait variables using computer vision to assess mobility and fall risk in older adults with dementia," *IEEE J. Transl. Eng. Health Med.*, vol. 8, 2020, Art. no. 2100609.

[12] M. Hao, K. Chen, and C. Fu, "Smoother-based 3-D foot trajectory estimation using inertial sensors," *IEEE Trans. Biomed. Eng.*, vol. 66, no. 12, pp. 3534–3542, Dec. 2019.

[13] J. Hannink *et al.*, "Mobile stride length estimation with deep convolutional neural networks," in *Proc. IEEE J. Biomed. Health Inform.*, vol. 22, no. 2, pp. 354–362, Mar. 2018.

[14] N. Kitagawa and N. Ogihara, "Estimation of foot trajectory during human walking by a wearable inertial measurement unit mounted to the foot," *Gait Posture*, vol. 45, pp. 110–114, Mar. 2016.

[15] T. Kagawa, T. Kato, and Y. Uno, "On-line control of continuous walking of wearable robot coordinating with user's voluntary motion," in *Proc. IEEE/RSJ Int. Conf. Intell. Robots Syst. (IROS)*, Sep. 2015, pp. 5321–5326.

[16] K. Zhang *et al.*, "Foot placement prediction for assistive walking by fusing sequential 3D gaze and environmental context," *IEEE Robot. Autom. Lett.*, vol. 6, no. 2, pp. 2509–2516, Apr. 2021.

[17] S. Sahoo, S. K. Panda, D. K. Pratihar, and S. Mukhopadhyay, "Prediction of step length using neuro-fuzzy approach suitable for prosthesis control," *IEEE Trans. Instrum. Meas.*, vol. 69, no. 8, pp. 5658–5665, Aug. 2020.

[18] Y. Wang and M. Srinivasan, "Stepping in the direction of the fall: The next foot placement can be predicted from current upper body state in steady-state walking," *Biol. Lett.*, vol. 10, no. 9, p. 20140405, 2014.

[19] T. Koolen, T. de Boer, J. Rebula, A. Goswami, and J. Pratt, "Capturability-based analysis and control of legged locomotion, Part 1: Theory and application to three simple gait models," *Int. J. Robot. Res.*, vol. 31, no. 9, pp. 1094–1113, 2012.

[20] J. Luo, Y. Zhao, L. Ruan, S. Mao, and C. Fu, "Stimation of CoM and CoP trajectories during human walking based on a wearable visual odometry device," *IEEE Trans. Autom. Sci. Eng.*, early access, Nov. 20, 2020, doi: 10.1109/TASE.2020.3036530.

[21] Y. Wang, A. Chernyshoff, and A. M. Shkel, "Study on estimation errors in ZUPT-aided pedestrian inertial navigation due to IMU noises," *IEEE Trans. Aerosp. Electron. Syst.*, vol. 56, no. 3, pp. 2280–2291, Jun. 2020.

[22] R. Van De Schoot *et al.*, "Bayesian statistics and modelling," *Nature Rev. Methods Primers*, vol. 1, no. 1, pp. 1–26, 2021.

[23] X. Chen and J. Huang, "Combining particle filter algorithm with bio-inspired anemotaxis behavior: A smoke plume tracking method and its robotic experiment validation," *Measurement*, vol. 154, Mar. 2020, Art. no. 107482.

[24] X. Chen, A. Marjovi, J. Huang, and A. Martinoli, "Particle source localization with a low-cost robotic sensor system: Algorithmic design and performance evaluation," *IEEE Sensors J.*, vol. 20, no. 21, pp. 13074–13085, Dec. 2020.

[25] U. Martínez-Hernandez and A. A. Dehghani-Sanij, "Adaptive Bayesian inference system for recognition of walking activities and prediction of gait events using wearable sensors," *Neural Netw.*, vol. 102, pp. 107–119, Jun. 2018.

[26] J. R. Rebula, L. V. Ojeda, P. G. Adamczyk, and A. D. Kuo, "Measurement of foot placement and its variability with inertial sensors," *Gait Posture*, vol. 38, no. 4, pp. 974–980, 2013.

[27] L. Zhang and C. Fu, "Predicting foot placement for balance through a simple model with swing leg dynamics," *J. Biomechanics*, vol. 77, pp. 155–162, Aug. 2018.

[28] R. T. Marler and J. S. Arora, "Function-transformation methods for multi-objective optimization," *Eng. Optim.*, vol. 37, no. 6, pp. 551–570, Sep. 2005.

[29] A. Peruzzi, U. Della Croce, and A. Cereatti, "Estimation of stride length in level walking using an inertial measurement unit attached to the foot: A validation of the zero velocity assumption during stance," *J. Biomech.*, vol. 44, no. 10, pp. 1991–1994, Jul. 2011.

[30] S. Ahmed, H. Wang, and Y. Tian, "Model-free control using time delay estimation and fractional-order nonsingular fast terminal sliding mode for uncertain lower-limb exoskeleton," *J. Vib. Control*, vol. 24, no. 22, pp. 5273–5290, Dec. 2018.

[31] D. M. Ka, C. Hong, T. H. Toan, and J. Qiu, "Minimizing human-exoskeleton interaction force by using global fast sliding mode control," *Int. J. Control, Autom. Syst.*, vol. 14, no. 4, pp. 1064–1073, 2016.

[32] K. Zhang *et al.*, "A subvision system for enhancing the environmental adaptability of the powered transfemoral prosthesis," *IEEE Trans. Cybern.*, vol. 51, no. 6, pp. 3285–3297, Jun. 2021.